Polymer Journal (2024) 56:215–220
https://doi.org/10.1038/s41428-023-00864-8

RAPID COMMUNICATION

Depth analysis of local conformation in poly(methyl methacrylate) adsorbed onto SiO_x studied by soft X-ray absorption spectroscopy combined with an Ar gas cluster ion beam

Hiroyuki Yamane[1,6] · Masaki Oura[1] · Daisuke Kawaguchi[2] · Kiyofumi Nitta[3] · Oki Sekizawa[3] · Tetsuya Ishikawa[1] · Satoru Yamamoto[4] · Keiji Tanaka[4,5] · Takaki Hatsui[1]

Received: 3 October 2023 / Revised: 13 November 2023 / Accepted: 13 November 2023 / Published online: 25 December 2023

Abstract

Using X-ray absorption spectroscopy (XAS) with linearly polarized soft X-rays, we investigated the local conformation of poly(methyl methacrylate) (PMMA) adsorbed to a SiO_x/Si(111) surface. The preedge intensity of the O K-edge XAS for PMMA, originating from the O 1s → π^* transition at a C=O group in the side chain, was stronger for vertically polarized incident X-rays than for horizontally polarized ones. Conversely, the XAS intensity originating from the O 1s → σ^* transition showed the opposite trend. These findings suggest that the C=O group in the side chain of PMMA exhibited preferential orientation rather than an amorphous arrangement. To gain further insights, we conducted a depth profile analysis of the local conformation of PMMA using XAS combined with an argon gas cluster ion beam (GCIB). GCIB-XAS analysis revealed that the orientation of the C=O group in the side chain of PMMA differs between the region from the SiO_x interface to a distance on the order of 1 nanometer and the bulk PMMA region.

Introduction

Adhesion is a fundamental and essential technique in various applications, including polymer composites. It is well known that physical and chemical interactions in adhesives, adherends, and their interfaces determine the adhesive strength. The reliability of adhesion technology has been discussed based on macroscopic failure analysis due to tensile, compressive, shear, and peel stress responses [1]. At the microscopic level, the adhesive strength is determined by the complex interplay of chemical bonding, electrostatic forces, and molecular diffusion/entanglement [1]. The aggregation states from the interface to the bulk of the adhesive/adherend can be the key to unraveling adhesion at the molecular level, and the interfacial conformation of polymers has been discussed using sum-frequency generation (SFG) spectroscopy [2–4]. Spectroscopic depth analysis of adhesion structures offers a promising approach to differentiate the conformational structure from the bulk to the interface.

A gas cluster ion beam (GCIB) is composed of several thousand gas atoms that allow ion beam etching at low energy per atom, which cannot be achieved with conventional sputtering techniques [5]. The use of GCIB enables us to perform spectroscopic depth analysis of soft matter.

Supplementary information The online version contains supplementary material available at https://doi.org/10.1038/s41428-023-00864-8.

✉ Hiroyuki Yamane
yamane@phosic.or.jp

✉ Takaki Hatsui
hatsui@spring8.or.jp

[1] RIKEN SPring-8 Center, RIKEN, Kouto, Sayo, Hyogo 679-5148, Japan

[2] Department of Chemistry and Biotechnology, Graduate School of Engineering, The University of Tokyo, Bunkyo-ku, Tokyo 113-8656, Japan

[3] Japan Synchrotron Radiation Research Institute, SPring-8, Kouto, Sayo, Hyogo 679-5198, Japan

[4] Centre for Polymer Interface and Molecular Adhesion Science, Kyushu University, Fukuoka819-0395Japan

[5] Department of Applied Chemistry, Kyushu University, Fukuoka 819-0395, Japan

[6] Present address: Photon Science Innovation Center, NanoTerasu, Aramaki Aoba, Sendai 980-0845, Japan

Indeed, the depth distribution of chemical species has been studied using X-ray photoelectron spectroscopy (XPS) and secondary ion mass spectrometry (SIMS) in combination with GCIB [6–9]; however, XPS and SIMS in principle do not provide insight into the conformational information.

Soft X-ray absorption spectroscopy (XAS) using synchrotron radiation is a technique for measuring the transition probability upon inner-shell excitation, which provides local chemical states at specific elements and functional groups in materials. Furthermore, the intensity of the XAS feature is determined by the transition probability for inner-shell electrons with polarized X-rays [10]. Therefore, the polarization dependence of XAS depends not only on the local chemical states but also on the local conformation. In the present work, we applied a new methodology, XAS in combination with GCIB (GCIB-XAS), to a polymer-silica model interface: poly(methyl methacrylate) (PMMA) films adsorbed onto Si(111) with a native oxide (SiO_x) layer. We were able to observe the polarization dependence in the O K-edge XAS feature of the C=O group in the side chain of PMMA as well as its depth dependence. Based on the analysis of the XAS feature, we discuss the depth dependence of the local conformation of PMMA adsorbed onto the SiO_x/Si(111) surface. The observed data demonstrated that the orientation analysis using XAS in combination with GCIB allows depth analysis of the conformation with high resolution, which has not been elucidated experimentally.

Experimental

PMMA was purchased from Polymer Source Inc.. The number-average molecular weight (M_n) and molecular weight distribution (M_w/M_n) were 300 k and 1.05, respectively, where M_w is the weight-average molecular weight. The chain dimension, corresponding to twice the radius of gyration ($2R_g$), was calculated to be 30.0 nm. The glass transition temperature of PMMA was determined to be 400 K based on differential scanning calorimetry at a heating rate of 10 K·min^{-1}. We prepared PMMA films on a SiO_x/Si(111) substrate by a spin coating method. The prepared samples are listed in Table 1. PMMA samples 1 and 2–5 were coated at 3000 rpm for 60 s from toluene solutions of 2.0 wt% and 0.6 wt%, respectively. The PMMA/SiO_x/Si(111) samples were annealed at 423 K for several annealing times (0, 0.5, 12, and 24 h) to promote conformational relaxation. After thermal annealing, the samples were introduced into the GCIB-XAS system maintained under ultrahigh vacuum.

We performed the XAS measurements at the soft X-ray undulator beamline BL27SU of SPring-8 [11]. The XAS measurement system consisted of a silicon drift detector (XR100SDD, Amptek) and a GCIB source (GCIB 10, Ionoptika). The O K-edge XAS spectra were obtained based on the partial fluorescence yield method by measuring the O Kα fluorescent X-rays with a silicon drift detector. The angle of the incident direction of the X-ray beam was 70° with respect to the surface normal direction ($\boldsymbol{n}$), and horizontal and vertical polarization measurements with electric vectors of $\boldsymbol{E}_{\parallel}$ and $\boldsymbol{E}_{\perp}$, respectively, were performed in this XAS measurement configuration. The horizontally and vertically polarized incident X-rays were obtained with a high degree of polarization (P) of 0.98 by tuning a Figure-8 undulator [12, 13]. In the present work, the energy resolving power ($E/\Delta E$), photon flux, and beam size at the sample surface were 5000 at the O K-edge, on the order of 10^{11} ph/sec, and less than 0.5 mmφ, respectively. For the GCIB treatment, Ar 1000 clusters with a bias voltage of 5 kV were introduced to the sample surface at an incident angle of 75° with respect to the surface normal direction. Using a raster scan of GCIB, the etched area was a 2 mm square on the sample surface. The etch rate was approximately 0.16 nm/min (see Supplementary Information). XAS measurements and GCIB treatment were performed at room temperature.

Table 1 List of the PMMA/SiO_x/Si(111) samples in the present work

Sample name	Thickness	Annealing time at 423 K	Experimental data
PMMA-1	96 nm	24 hours	Fig. 2
PMMA-2	18 nm	N/A	Fig. 3
PMMA-3	18 nm	0.5 hours	Fig. 3
PMMA-4	18 nm	12 hours	Fig. 3
PMMA-5	18 nm	24 hours	Figs. 3 and 4

Molecular dynamics (MD) simulations were conducted using the Forcite module of Materials Studio 2023 (Dassault Systèmes) with the COMPASSIII force field to examine the detailed atomistic structure of PMMA on a quartz substrate. The substrate was prepared by using a SiO_2 crystal structure with a thickness of 3 nm and a surface of 5×5 nm^2, capped with OH groups. The initial model was created by sandwiching five syn-PMMA chains with a molecular weight of 15k at a density of 1.02 g·cm^{-3} between the quartz surfaces with a 5 nm gap through a periodic boundary. A total of six interfaces were evaluated for three different initial models after MD simulations at 298 K for 1 ns.

Results and discussion

Figure 1 shows the O K-edge XAS spectra for PMMA-1 as a function of the number of scans. The X-ray beam used was horizontally polarized. The XAS spectra showed a sharp preedge peak at an incident photon energy (hv) of 532.0 eV. According to previous studies [14–16], the

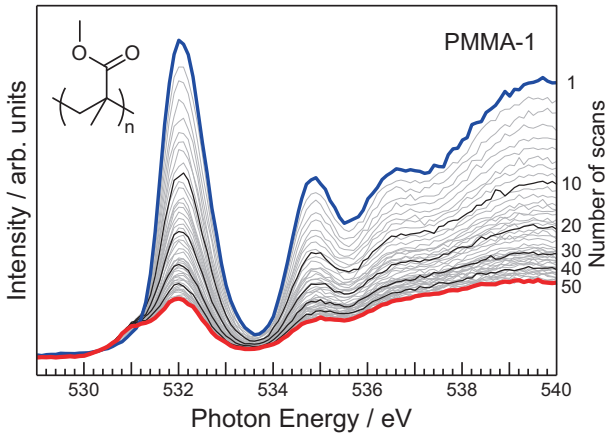

Fig. 1 O K-edge XAS spectra for PMMA-1 as a function of the number of scans (50 scans in total). First and last scan data are indicated by blue and red curves, respectively. The chemical structure of PMMA is shown in the inset

preedge peak and next XAS peak at 534.9 eV were attributed to the O 1s → π^* transitions at the C=O site in PMMA, and other broad XAS features at $h\nu > 536$ eV were attributed to the O 1s → σ^* transitions. As the number of scans increased, the XAS spectral intensity became weaker, with a shoulder feature appearing on the low $h\nu$ side ($h\nu = 530.9$ eV). The decrease in XAS intensity can be explained by mass loss associated with photoionization [15, 16]. The shoulder structure at $h\nu = 530.9$ eV results from the formation of damage-induced chemical species at the OH site in the side chain of PMMA [17]. Notably, although the GCIB treatment has been considered to be a damage-free etching method, we found that the XAS spectra of the PMMA sample showed a damage-induced peak at $h\nu =$ 530.9 eV depending on the incident angle and bias voltage of GCIB. Such damage could lead to the formation of new chemical bonds and a possible change in conformation. In the following GCIB-XAS measurements, we minimized the GCIB-induced chemical change by using the wide incident angle of GCIB with respect to the surface normal direction of 75° and the low bias voltage of 5 kV (see Supplementary Information).

Figure 2a shows the O K-edge XAS spectra for PMMA-2 measured with horizontally and vertically polarized incident X-rays, where the spectra were normalized to the intensity in the postedge region ($h\nu = 546$ eV). The π^* feature ($h\nu = 530$~535 eV) appeared stronger with vertical polarization than with horizontal polarization, while the σ^* feature ($h\nu > 536$ eV) appeared weaker. The observed polarization dependence can be explained by the different transition probabilities for the π^* and σ^* orbitals with the electric vector of linearly polarized X-rays. Furthermore, we found that the polarization dependence of XAS was weakened upon annealing, as shown in the inset of Fig. 2a. These features are reflected in the difference curve of the vertical XAS data minus the horizontal XAS data (hereafter XAS_{V-H}), as shown in Fig. 2b. The intensity of the XAS_{V-H} spectra for annealed PMMA (PMMA-3, 4, and 5) was weaker than that for as-prepared PMMA (PMMA-2) and exhibited slight changes with annealing time. It should be noted that the present XAS spectra directly probed the local chemical state around the C=O group in the side chain of PMMA but not the main chain. The change in the XAS feature upon annealing was attributed to the change in the orientation of the C=O group, which can be attained by the conformational relaxation of the main and side chains of PMMA.

We discuss the orientation angle (β) of the C=O group in the side chain of PMMA from the XAS intensity ratio at two different polarization directions. Here, β is defined as the angle between the C=O bond vector to normal to the substrate surface. As shown in Fig. 2a, the incident X-rays were linearly polarized with the electric vectors oriented along the horizontal or vertical direction. It is known that the XAS intensity (I) is governed by the interaction between the electric vector of the incident X-rays ($\boldsymbol{E}$) and the transition dipole moment ($\boldsymbol{p}$); $I \propto |\boldsymbol{Ep}|^2$ [10]. In the case of the 1s → π^* resonance at the C=O group, the dipole moment is oriented perpendicular to the bond direction. Analyzing XAS data in relation to the polarization angle enables a quantitative determination of β. The relationship between β and the XAS intensities [$I(\alpha_1)$ and $I(\alpha_2)$] is given by the following equation after azimuthal averaging, where α_1 and α_2 denote the angles between the electric vector of the incident X-rays and the surface normal [10].

$$\tan^2\beta = \frac{1}{2P}\left(P - \frac{1 - \frac{I(\alpha_2)}{I(\alpha_1)}}{\sin^2\alpha_2 - \frac{I(\alpha_2)}{I(\alpha_1)}\sin^2\alpha_1}\right) \quad (1)$$

In XAS measurements, the upward or downward direction of the C=O bond vector cannot be distinguished, resulting in β values ranging from 0 to 90°. The high degree of polarization at SPring-8 BL27SU ($P = 0.98$) [12, 13] allows us to consider the angle between the electric vector and the surface normal to be $\alpha_1 = 0°$ for the vertical polarization measurement and $\alpha_2 = 70°$ for the horizontal polarization. The intensity ratio $I(\alpha_2)/I(\alpha_1)$ can be determined from the raw XAS data shown in Fig. 2a. From the XAS intensity analysis, we found that the C=O group in the side chain of PMMA was oriented at an average of $\beta = 33.8°$ for PMMA-2 (as-prepared PMMA) and $\beta = 34.5$~$34.6°$ for PMMA-3, 4, and 5 (annealed PMMA).

It was reported using SFG that ester methyl groups of PMMA on SiO_x were oriented along the surface normal direction due to the interaction via hydrogen bonding between carbonyl groups of PMMA and the substrate surface [4]. In the present work, the determined β of less than 45° indicates that the C=O groups were relatively oriented

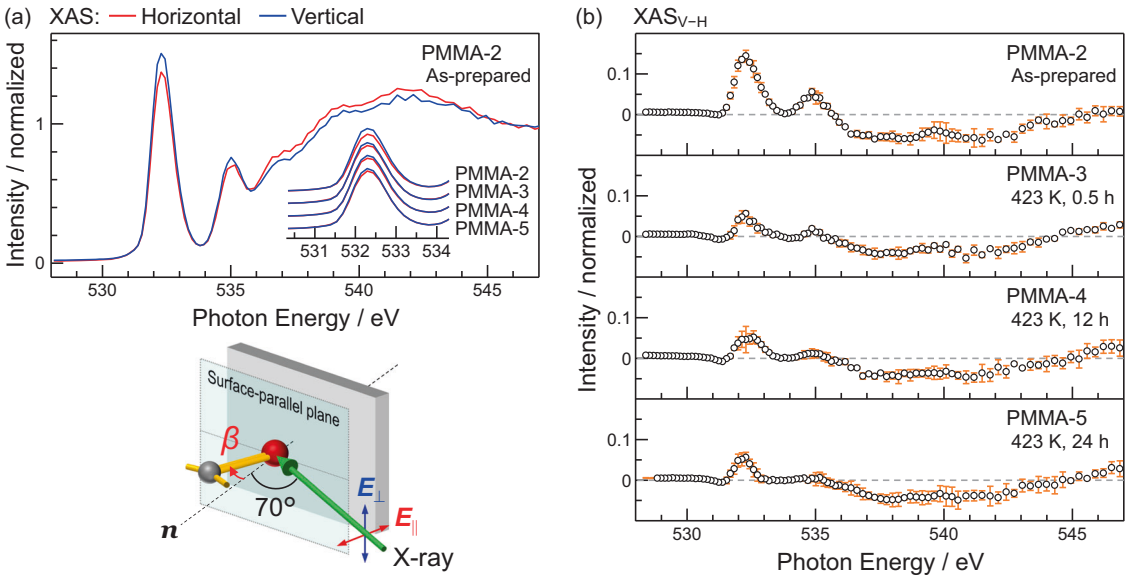

Fig. 2 **a** O K-edge XAS spectra for PMMA-2 measured with horizontally and vertically polarized incident X-rays. Preedge peaks for PMMA-2, 3, 4, and 5 are shown in the inset. A schematic illustration of the XAS measurement geometry is also shown. The orientation angle β is measured from the surface normal direction (***n***). **b** Annealing time dependence of the difference spectra (vertical minus horizontal) shown with error bars

along the surface normal direction rather than along the substrate surface. On the other hand, the film thicknesses for PMMA-2, 3, 4, and 5 to be 18 nm were smaller than $2R_g$, indicating that the PMMA chains were in a confined state. In other words, while the main chain was relatively oriented parallel to the substrate surface, the side groups were oriented perpendicular to the substrate surface. These results are consistent with those of a previous study using SFG [4].

To discuss the depth distribution of the local conformation of PMMA-5, we performed O K-edge XAS measurements combined with GCIB treatment, which was performed by increasing the GCIB exposure time while keeping the other parameters unchanged. Figure 3a shows the O K-edge XAS spectra, in which the vertical and horizontal polarization data were summed as a function of the number of GCIB treatments (labeled GCIB 0~7). As the GCIB treatment times increased, the intensity of the XAS feature decreased due to the reduction in PMMA thickness. For the 5- and 6-time treated samples (GCIB 5 and 6, respectively), the XAS feature at $h\nu > 536$ eV became stronger than that at $h\nu = 531$~536 eV. This originated from the increase in the contribution of the SiO_x/Si(111) substrate due to the probing depth of soft X-rays. For GCIB 7, the PMMA-derived XAS feature disappeared and showed the characteristics of SiO_2 [18, 19]. From the GCIB treatment times and spectral shape, the nominal thickness of the GCIB-treated PMMA-5 sample was determined to be 18 nm (for GCIB 0), 16 nm (GCIB 1), 15 nm (GCIB 2), 12 nm (GCIB 3), 10 nm (GCIB 4), 6 nm (GCIB 5), 1 nm (GCIB 6), and 0 nm (GCIB 7). We noted that while the spectral intensity changed with sample thickness, no additional XAS peak was observed. This evidence indicated the absence of interfacial covalent bonding between PMMA and SiO_x/Si(111).

Figure 3b shows the XAS_{V-H} spectra of PMMA-5 as a function of GCIB treatment. Before obtaining the XAS_{V-H} spectra, the intensities of the vertical and horizontal XAS data were normalized to the postedge region. Although the signal intensity was weak, the XAS_{V-H} spectra showed depth dependence. The intensity of the polarization dependence was reduced for GCIB 5 and absent for GCIB 6 [1-nm-thick PMMA on SiO_x/Si(111)] and 7 [SiO_x/Si(111)]. The results imply that the orientation of the C=O groups at a depth of 1 nm from the substrate was different from that in the upper region of the film. Here, if the roughness and morphology existed on the sample after the GCIB treatment, the spectral shape, signal intensity, and polarization dependence in XAS should depend on the measurement position. In the present experiment, the spot size of the incident X-rays was approximately 200 μm square, which was small with respect to the GCIB treatment area of 2 mm square. By measuring XAS at different measurement positions on the sample, we found no evidence for roughness and morphology after GCIB treatment within the present spatial resolution.

To discuss the orientation of C=O groups at the outermost substrate interface, an MD simulation was conducted. In the MD simulation, where the upward or downward direction can be distinguished, β values will range from 0 to 180° hereafter. Before going to the MD results, the number of C=O groups oriented in the range from β to $\beta + \Delta\beta$ is defined as $n(\beta)$. Postulating that the orientation of C=O

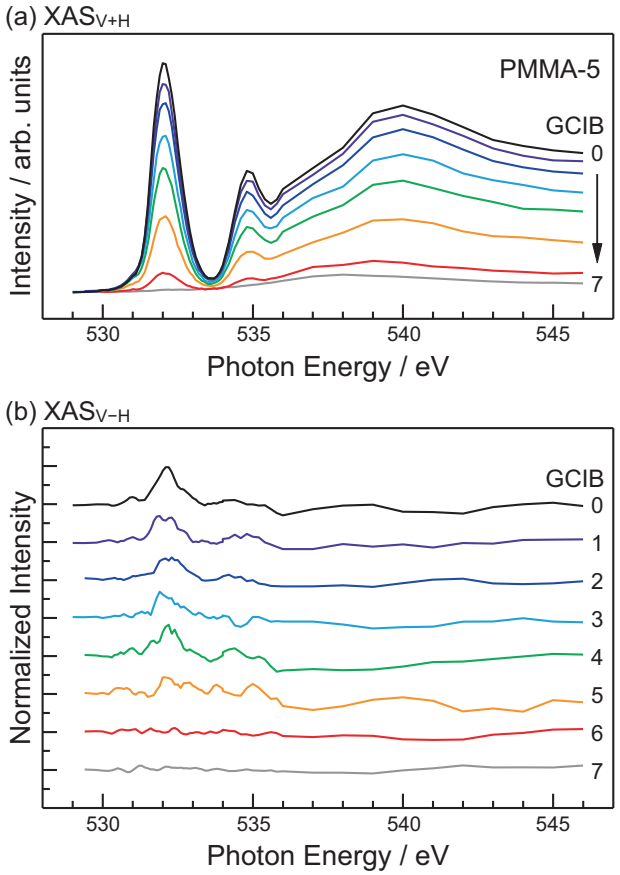

Fig. 3 O K-edge XAS spectra as a function of GCIB treatment for PMMA-5. The number of GCIB treatments is indicated by 0~7, where 0 is the as-prepared PMMA-5 sample. **a** The summed XAS spectra of the vertical and horizontal polarization data. **b** The XAS$_{V-H}$ spectra of the vertical minus horizontal polarization data

groups is isotropic, the possibility of finding the C=O groups can be described as

$$\frac{n(\beta)}{N}\Delta\beta = \frac{2\pi r^2 \sin\beta}{4\pi r^2}\Delta\beta = \frac{1}{2}\sin\beta\Delta\beta \qquad (2)$$

where r is the arbitrary radius of the circle. N is the total number of C=O groups contained in a circle with r. Therefore, a sine function-like distribution indicates the random orientation of C=O groups. Figure 4 shows the distribution of β in the depth range from 0 to 0.5 nm. This deviation was from a sine function, and the peaks appeared ca. 30 and 120°. This implied that the C=O groups were preferentially oriented at the outermost substrate interface. On the other hand, there are three possibilities to explain the absence of polarization dependence in the XAS intensity for GCIB 6: (1) the random orientation, (2) the magic angle orientation, and (3) the multiple orientations. Taking into account the results of the MD calculation, the random orientation of C=O groups is unlikely. The magic angle gives the XAS intensity independent of the X-ray incident angle. In this case, β is 35.26° due to $I(\alpha_2)/I(\alpha_1) = 1$ in Eq. (1). On the other hand, multiple orientations broaden the

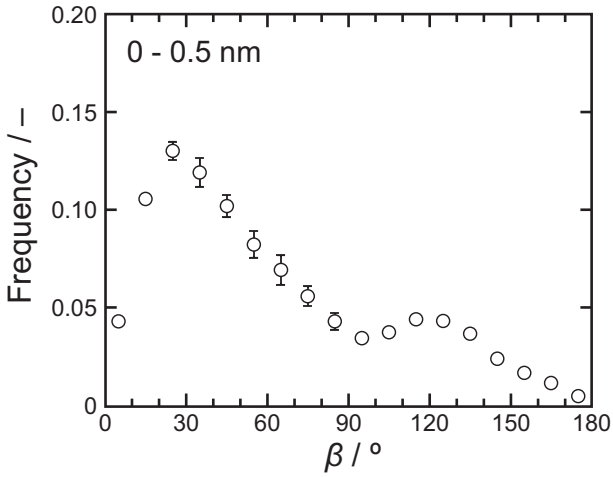

Fig. 4 Orientation angle distribution of C=O groups in the depth region of 0~0.5 nm

polarization dependence. Although the possibilities of magic-angle and multiple orientations are suggested by the present MD calculation, we could not give a definite interpretation of the XAS feature of GCIB 6 in the present work. These possibilities can be examined by soft X-ray imaging using a focused X-ray beam, which can visualize the spatial distribution of domain orientation and molecular order of polymers.

Conclusion

We investigated the depth distribution of the local conformation of PMMA adsorbed onto SiO_x/Si(111). For this purpose, we applied the XAS measurements combined with Ar-GCIB. The XAS features exhibited polarization dependence, where the π^* transition peak at the C=O group in the side chain of PMMA was stronger for vertically polarized incident X-rays than for horizontally polarized incident X-rays. The observed polarization dependence of XAS allowed us to discuss the change in the local conformation of the C=O group in the side chain of PMMA due to the structural relaxation induced by annealing at 423 K. From the depth-dependent polarization dependence of XAS, we were also able to discuss the depth distribution of the local conformation of PMMA. We found that the local conformation of PMMA in the 1 nm region from the SiO_x interface is different from that of bulk PMMA.

Acknowledgements HY, MO, and TH are grateful to Professor Yusuke Tamenori (Tokyo Metropolitan University) for the discussion of the experimental setup at BL27SU of SPring-8. This work was supported by the JST-Mirai Program (JPMJMI18A2). HY acknowledges financial support from JSPS (20H02702). The GCIB-XAS experiments at BL27SU of SPring-8 were conducted with the approval of the Japan Synchrotron Radiation Institute (Proposal No. 2021A1036).

Compliance with ethical standards

Conflict of interest The authors declare no competing interests.

Publisher's note Springer Nature remains neutral with regard to jurisdictional claims in published maps and institutional affiliations.

References

1. Troughton MJ. Handbook of plastics joining: a practical guide. NY: William Andrew; Elsevier; 2008.
2. Abe T, Shimada H, Hoshino T, Kawaguchi D, Tanaka K. Sum frequency generation imaging for semi-crystalline polymers. Polym J. 2022;54:679–85.
3. Uchida K, Mita K, Yamamoto S, Tanaka K. Conformational relaxation of ethylene-propylene-diene terpolymer at a solid interface. Polym J. 2023;55:683–90.
4. Inutuka M, Horinouchi A, Tanaka K. Aggregation states of polymers at hydrophobic and hydrophilic solid interfaces. ACS Macro Lett. 2015;4:1174–8.
5. Yamada I, Matsuo J, Toyoda N, Lirkpatrick A. Materials processing by gas cluster ion beams. Mater Sci Eng R. 2001;34:231–95.
6. Erickson NC, Raman SN, Hammond JS, Holmes RJ. Depth profiling organic light-emitting devices by gas-cluster ion beam sputtering and X-ray photoelectron spectroscopy. Org Electron. 2014;15:2988–92.
7. Shinohara T, Higaki Y, Nojima S, Masunaga H, Ogawa H, Okamoto Y, Aoki T, Takahara A. Molecular aggregation states and wetting behavior of a poly{2-(perfluorooctyl)ethyl acrylate} brush-immobilized nano-imprinted surface. Polymer. 2015;69:10–16.
8. Suzuki M, Nojima M, Fujii M, Seki T, Matsuo J. Mass analysis by Ar-GCIB-dynamic SIMS for organic materials. Surf Interface Anal. 2014;46:1212–4.
9. Sparvero LJ, Tian H, Amoscato AA, Sun WY, Anthonymuthu TS, Tyurina YY, Kapralov O, Javadov S, He RR, Watkins SC, Winograd N, Kagan VE, Bayır H. Direct mapping of phospholipid ferroptotic death signals in cells and tissues by gas cluster ion beam secondary ion mass spectrometry (GCIB-SIMS). Angew Chem. 2021;133:11890–4.
10. Stöhr J. NEXAFS spectroscopy. Berlin, Springer; 1992.
11. Ohashi H, Ishiguro E, Tamenori Y, Kishimoto H, Tanaka M, Irie M, Ishikawa T. Outline of soft X-ray photochemistry beamline BL27SU of SPring-8. Nucl Instrum Methods Phys Res A. 2001;467-468:529–32.
12. Tanaka T, Hara T, Oura M, Ohashi M, Kimura H, Goto S, Suzuki Y, Kitamura H. Construction and performance of a figure-8 undulator. Rev Sci Instrum. 1999;70:4153–60.
13. Yoshida H, Senba Y, Morita M, Goya T, Fanis AD, Saito N, Ueda K, Tamenori Y, Ohashi H. Polarization measurements of soft X-ray emitted from the Figure-8 undulator. AIP Conf Proc. 2004;705:267–70.
14. Tinone MCK, Tanaka K, Maruyama J, Ueno N, Imamura M, Matsubayashi N. Inner-shell excitation and site specific fragmentation of poly(methylmethacrylate) thin film. J Chem Phys. 1994;100:5988–95.
15. Beetz T, Jacobsen C. Soft X-ray radiation-damage studies in PMMA using a cryo-STXM. J Synchrotron Rad. 2002;10:280–3.
16. Wang J, Morin C, Li L, Hitchcock AP, Scholl A, Doran A. Radiation damage in soft X-ray microscopy. J Electron Spectrosc Relat Phenom. 2009;170:25–36.
17. Yamane H, Oura M, Takahashi O, Fons P, Varadwaj PR, Shimoi Y, Ohkubo M, Ishikawa T, Yamazaki N, Hasegawa K, Takagi K, Hatsui T. Soft X-ray absorption spectroscopy probes OH···π interactions in epoxy-based polymers. J Phys Chem C. 2020;120:9622–7.
18. Mo SD, Ching WY. X-ray absorption near-edge structure in alpha-quartz and stishovite: Ab initio calculation with core-hole interaction. Appl Phys Lett. 2001;78:3809–11.
19. Frati F, Hunault MOJY, de Groot FMF. Oxygen K-edge X-ray absorption spectra. Chem Rev. 2020;120:4056–110.